Electronic Supplementary Material (ESI) for Sensors & Diagnostics.

Supporting Information

Passivating Quantum Dots against Histag-Displaying Enzymes using Blocking Peptides: Salient Considerations for Self-Assembling Quantum Dot Biosensors

Christopher M. Green*, David A. Hastman, Kimihiro Susumu, Joseph Spangler, David A. Stenger, Igor L. Medintz, Sebastián A. Díaz*

Corresponding authors: christopher.green@nrl.navy.mil; sebastian.diaz@nrl.navy.mil

Materials. All blocking peptides were acquired from Bio-Synthesis in lyophilized form with trifluoroacetate (TFA) counter ions. The lyophilized peptides were rehydrated in molecular grade water and desalted to remove TFA. The desalted peptides were then rehydrated in 5% dimethylsulfoxide (DMSO) in water and diluted to a final stock concentration of 500 µM. QD520 and QD525 were synthesized in house using previously reported protocols and solubilized by ligand exchange with DHLA-CL4.[1, 2] QD625 was acquired from Thermo Fisher Scientific (Qdot 625 ITK carboxyl) and solubilized using the same ligand exchange protocol. Peptide-PNA was acquired from PNA Bio in lyophilized form and rehydrated to 50 µM in water. Cy3-labeled DNA and RNA oligos were acquired from Integrated DNA Technologies in desalted form and rehydrated to 100 µM in water. LwCas13a enzyme from *Leptotrichia wadei* was acquired from GenScript at 37.6 µM in 50 mM Tris-HCl with 500 mM NaCl, 5% glycerol, and 2 mM dithiolthreitol. Alkaline phosphatase was expressed and purified in-house using previously reported protocols.[3]

LwCas13a assay for RNA detection. LwCas13a assays were performed in 10 mM Tris-HCl (pH 8.0) with 10 mM $MgCl_2$ and 50 mM NaCl. LwCas13a enzyme and guide RNA (gRNA) were combined in equimolar ratios at 200 nM each and incubated at 37 ºC for 15 min to promote assembly of a Cas/gRNA ribonucleoprotein (RNP). A 35 nt target RNA in water was added to half of the Cas RNP solution at a ratio of 50 Cas RNP/target RNA and incubated at 37 ºC for 15 min to promote assembly of an activated Cas RNP/target complex. Water was added to the other half of the Cas RNP solution in place of target RNA. The Cas RNP and Cas RNP/target solutions were then split between 9 wells each (10 µL) in a 384-well plate. Three distinct reporter solutions were prepared in the same buffer described above and 10 µL was added to the Cas RNP and Cas RNP/target solutions in triplicate at the following concentrations: (1) 200 nM RNaseAlert v2 (RA), (2) 200 nM RA with 200 nM QD525, and (3) 200 nM RA with 200 nM QD525-BP (at 40 BP/QD). The 384-well plate was immediately covered with a transparent plate seal and loaded into a fluorescence plate reader preheated to 37 ºC, and fluorescence was measured over 1 h with excitation at 490 nm and emission at 520 nm.

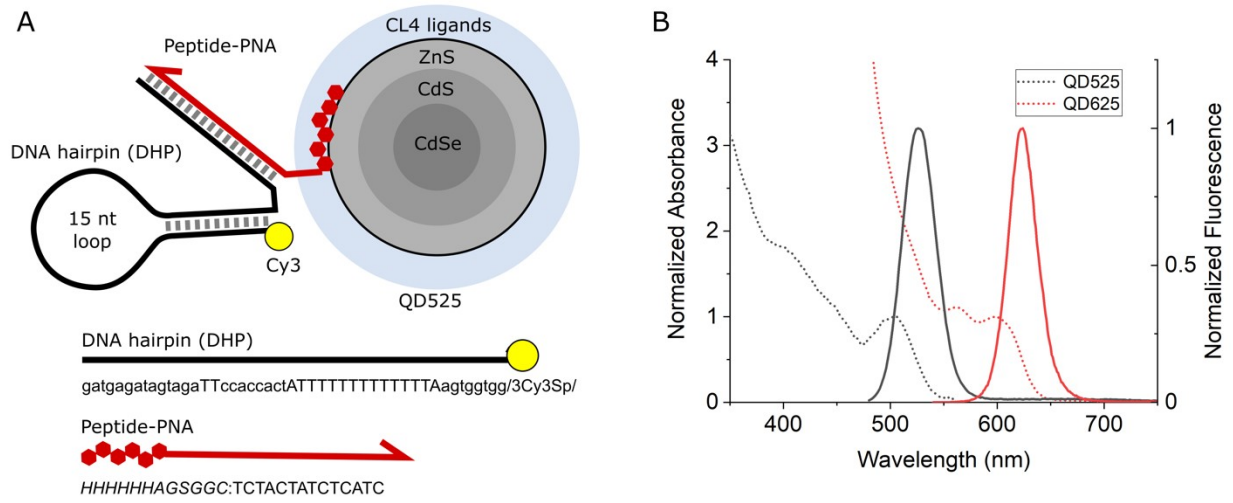

Figure S1 - (A) Schematic of QD molecular beacon, consisting of a chimeric peptide-PNA strand (red) hybridized to a DNA hairpin with 3' terminal Cy3 (DHP-Cy3, black). The peptide-PNA/DHP-Cy3 complex is bound to a CdSe/CdS/ZnS core/shell/shell QD by the histag of the peptide-PNA, which undergoes metal affinity coordination with Zn^{2+} on the QD surface. The DNA hairpin and peptide-PNA sequences (5'-3', N-C) are shown below the schematic. (B) Normalized absorbance and fluorescence spectra of QD525 (black) and QD625 (red).

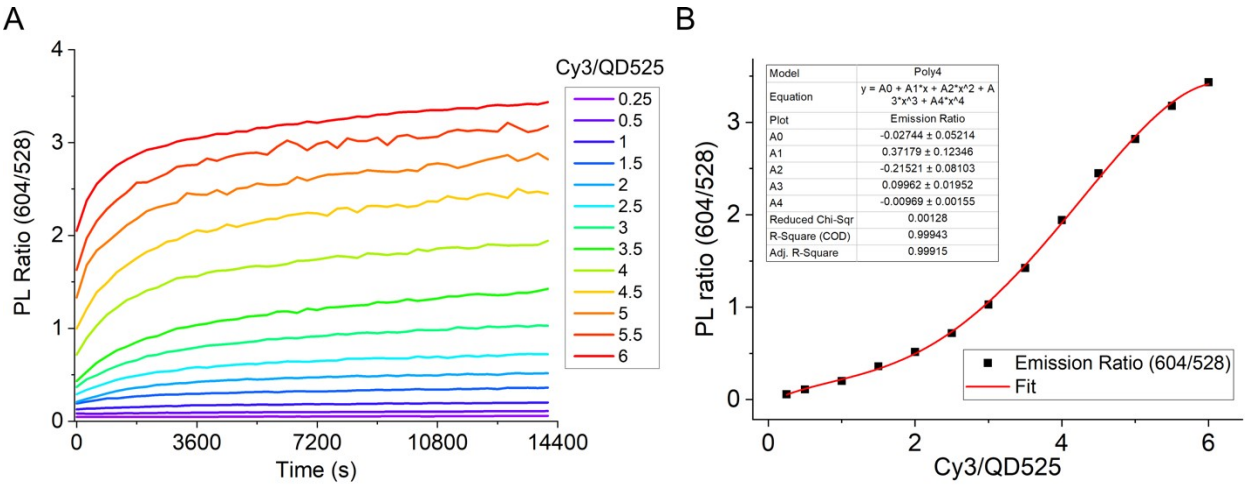

Figure S2 - (A) Kinetic trace of peptide-PNA:DHP-Cy3/QD525 complexes assembled at ratios of Cy3/QD525 varying from 0.25 to 6 at 100 nM QD525, run in parallel to samples in Figures S3 and S4 under identical conditions. (B) PL ratios at 4 h were used to generate a calibration curve to predict the number of Cy3 bound per QD525 from PL ratios for the samples tested. PL ratio vs ratio of Cy3/QD525 was fit with a fourth order polynomial for interpolation of BP titration data at 4 h, and this polynomial was used to generate the data presented in Figure 2c.

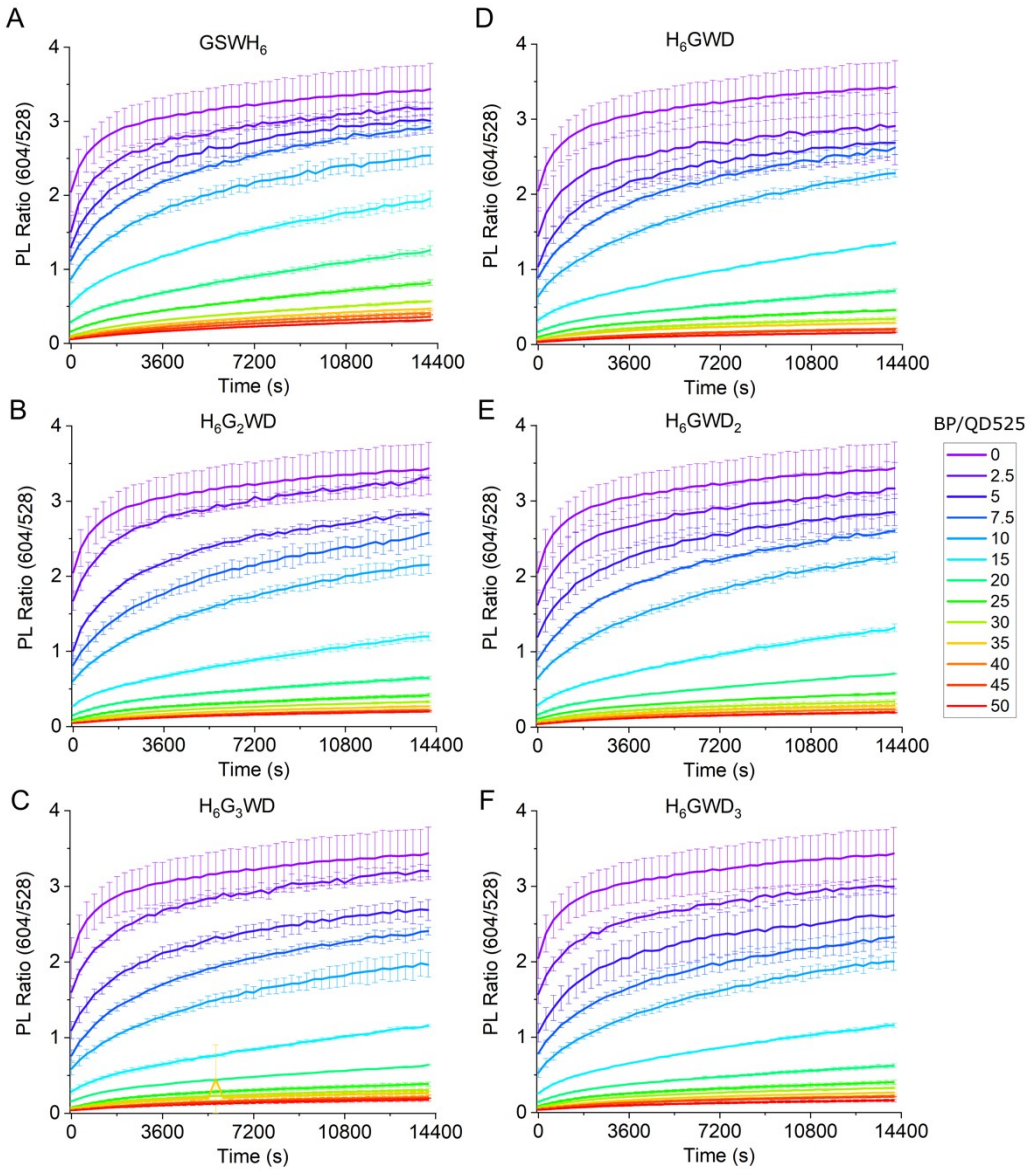

Figure S3 – Results of the titration of BPs $GSWH_6$ (A), H_6G_2WD (B), H_6G_3WD (C), H_6GWD (D), H_6GWD_2 (E), and H_6GWD_3 (F) with QD525 at ratios ranging from 0 to 50 BP/QD525 at 100 nM QD525 (final concentration) in 10 mM Tris-HCl (pH 8.0), 10 mM $MgCl_2$, and 50 mM NaCl. BPs and QD525 were allowed to assemble at room temperature for 1 h in a 384-well microplate. Peptide-PNA:DHP-Cy3 complexes were then added to each sample at a ratio of 6 Cy3/QD525, and the microplate was transferred to a plate reader for kinetic trace measurements over 4 h held at 25 ºC. Characterization was performed by excitation at 380 nm, and QD525 emission was measured at its peak emission (528 nm) while Cy3 emission was measured at 604 nm to minimize crosstalk with QD525. To quantify the conjugation of peptide-PNA:DHP-Cy3 complexes to QD525, the PL ratio was calculated from the emission of Cy3 relative to QD525 at 604 nm and 528 nm, respectively. At 4 h, samples with low ($\leq$ 5) and high ($\geq$ 30) BP/QD525 ratios approached a plateau in the PL ratio, and samples with BP/QD525 ratios between those values continued to increase steadily, suggesting an equilibrium had not yet been reached. Fluorescence spectra were acquired for all samples after 4 h and are provided in Figure S4.

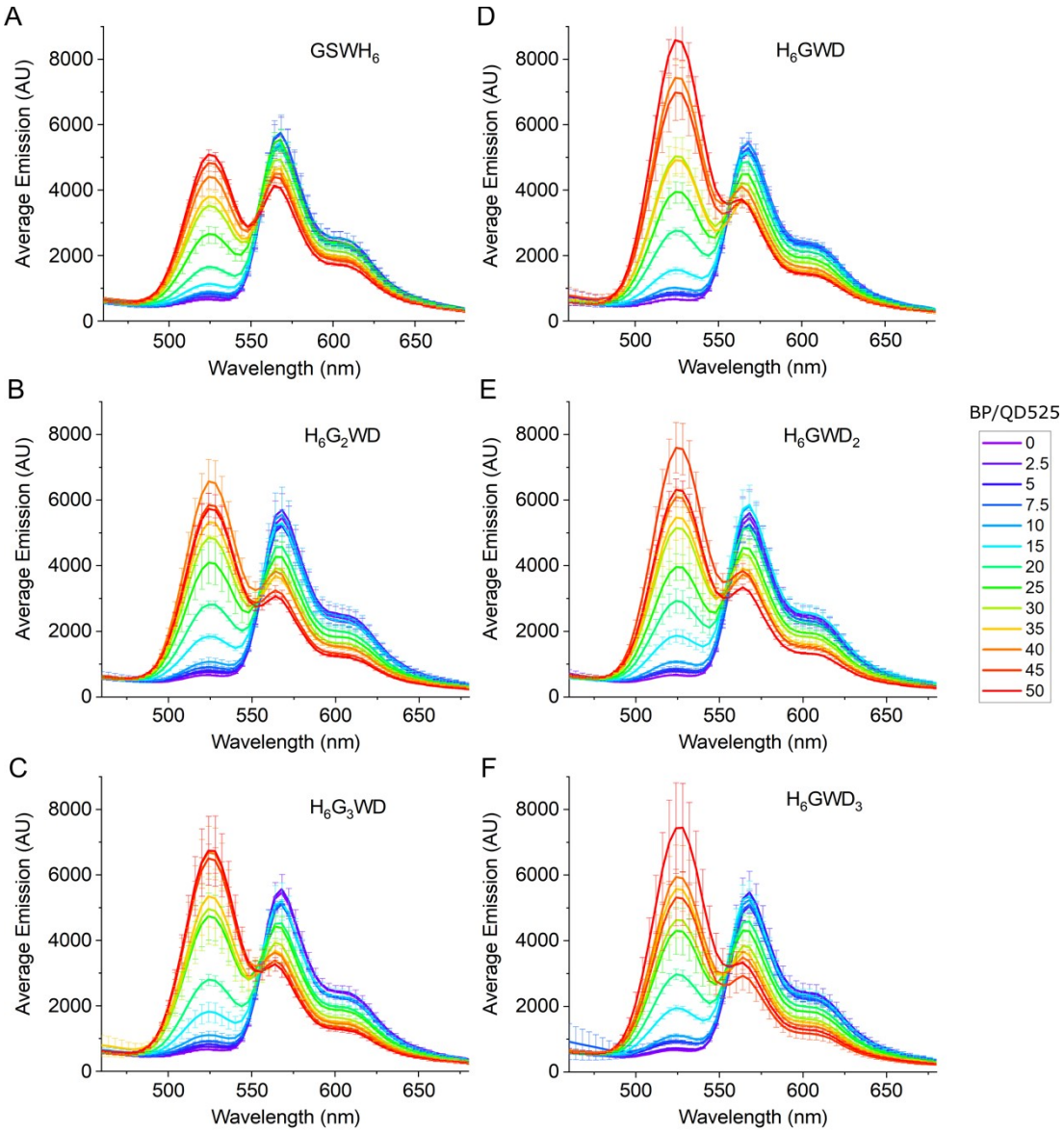

Figure S4 - Fluorescence spectra of peptide-PNA:DHP-Cy3 and BP-passivated QD525 mixtures at 6 Cy3/QD525 after 4 h kinetic trace measurements (shown in Figure S3). QD525 was pre-passivated with BPs $GSWH_6$ (A), H_6G_2WD (B), H_6G_3WD (C), H_6GWD (D), H_6GWD_2 (E), and H_6GWD_3 (F) at ratios ranging from 0 to 50 BP/QD525 prior to the addition of the Cy3 complexes. In the absence of BPs (purple – 0 BP/QD525), the Cy3 emission peak at 572 nm is significantly greater than the QD525 emission peak at 528 nm, indicating the conjugation of multiple Cy3 complexes to the surface of QD525 which resulted in Förster resonance energy transfer (FRET) between QD525 and Cy3. The result of FRET between QD525 and Cy3 is observed as quenching of QD525 and sensitization of Cy3. Direct excitation of Cy3 at 380 nm is negligible. For all BPs tested, increases in the ratios of BP/QD525 resulted in increased QD525 fluorescence and decreased Cy3 fluorescence, indicative of decreasing Cy3/QD525 conjugation.

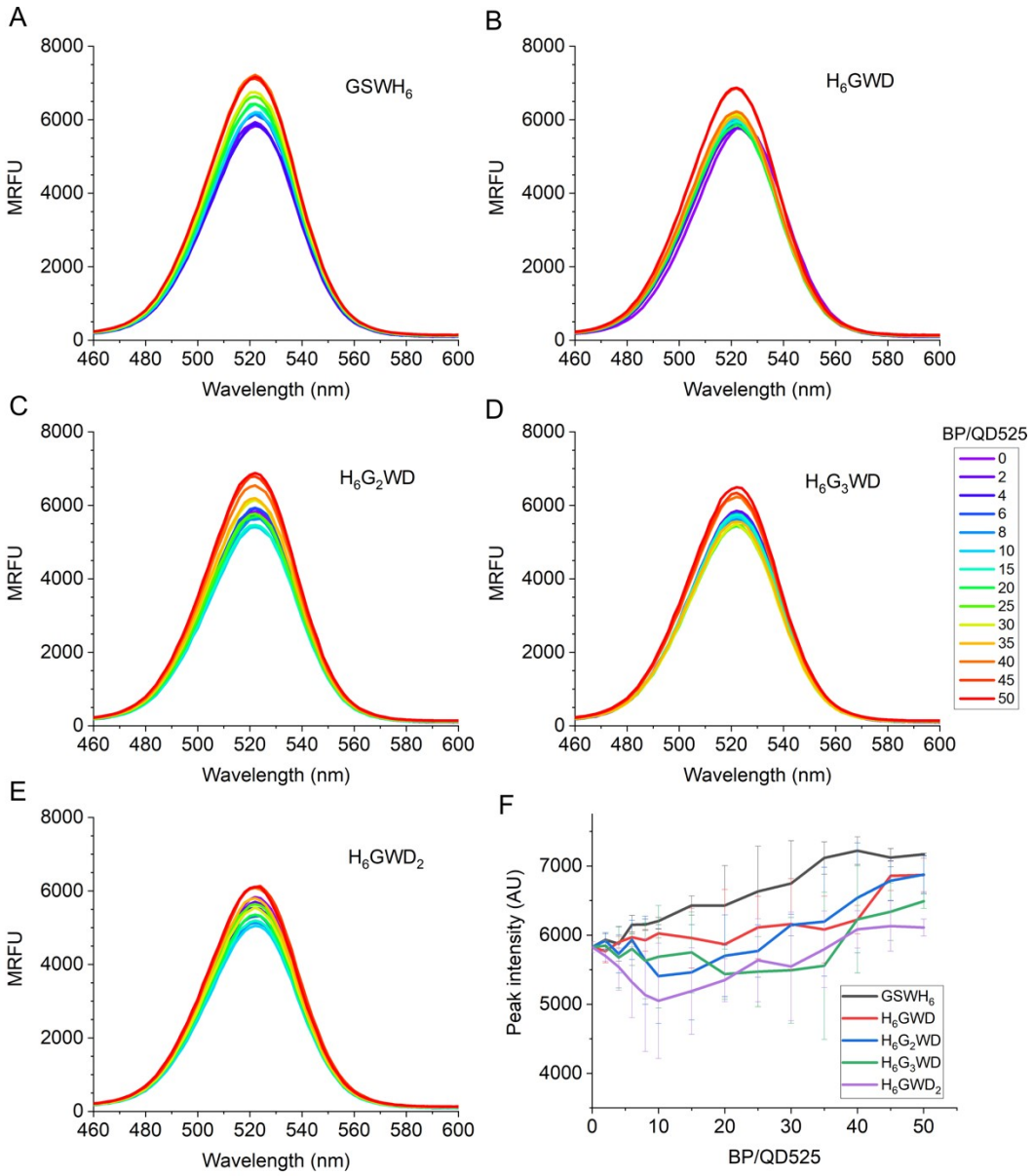

Figure S5 – Emission spectra of QD525 with varying ratios of BP/QD525 for BPs $GSWH_6$ (A), H_6GWD (B) H_6G_2WD (C), H_6G_3WD (D), and H_6GWD_2 (E). (F) Plot of peak emission intensity vs ratio of BP/QD525 for the samples shown in A-E. There is a slight increase in the intensity of emission with increasing BP/QD525 ratios.

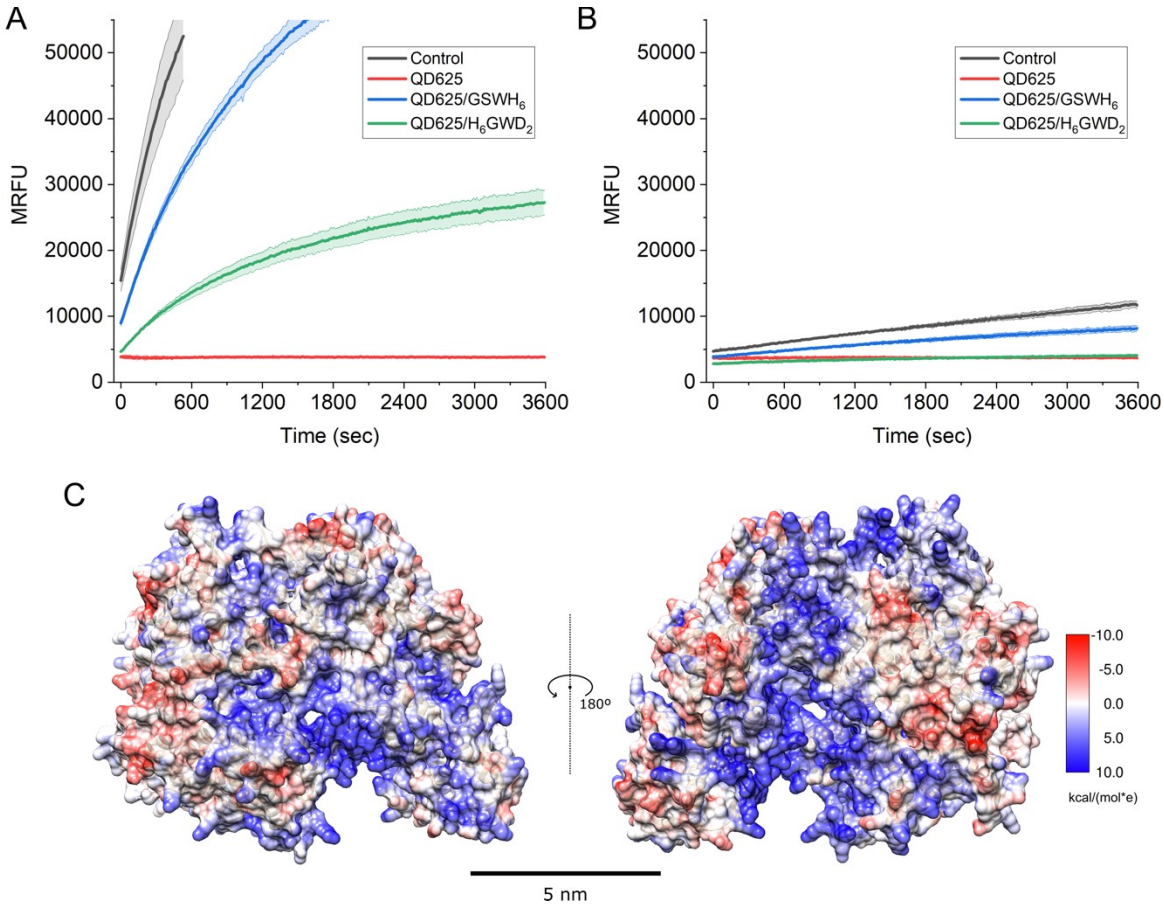

Figure S6 –LwCas13a-based RNA detection assays with (A) and without (B) 1 nM of target RNA. All samples contained 100 nM LwCas13a, 100 nM gRNA, and 200 nM RA in 10 mM Tris-HCl pH 8.0, 10 mM $MgCl_2$, and 50 mM NaCl. 1 nM of target RNA was added to each sample in (A), and samples with QD625 and blocking peptides had 100 nM QD625 and 10 µM of BPs. (C) AlphaFold model of LwCas13a (AF-U2PSH1-F1)[4, 5] with coulombic surface coloring to indicate the predicted electrostatic potential at the surface of the protein.

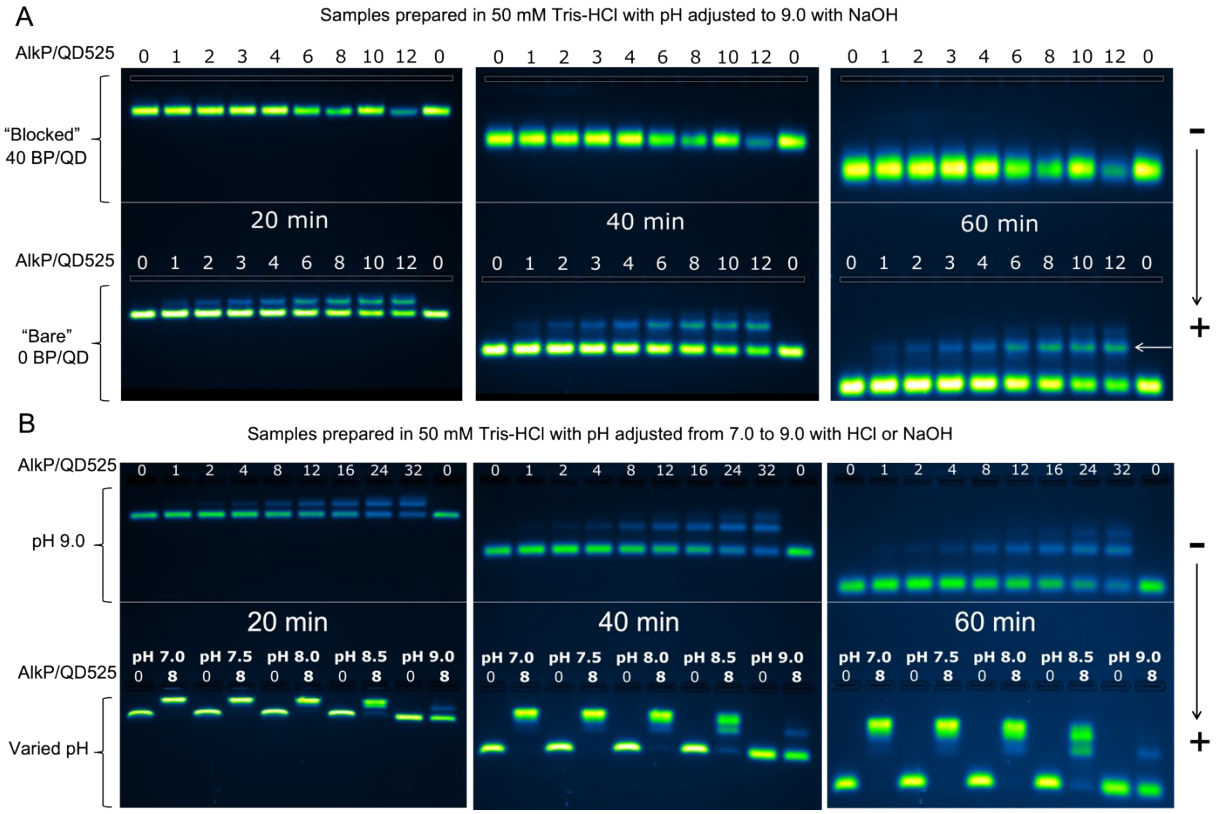

Figure S7 – Agarose gel electrophoretic mobility shift assays (EMSA) of AlkP/QD525 conjugates with blocking peptide H_6GWD_2. (A) Psuedocolor EMSA images of QD525 blocked with 40 BP/QD (top) and without BPs (bottom) prior to the addition of AlkP at ratios varying from 0 to 12 AlkP/QD. Samples were prepared in 50 mM Tris-HCl pH 9.0 and run in a 1.5% agarose gel with 1× TBE buffer at 7 V/cm. Images were taken at 20 min (left), 40 min (middle), and 60 min (right). For QDs blocked with BPs, only a single band was observed that corresponded to QDs without AlkP, indicating that AlkP conjugation to QDs was prevented. For bare QDs, a low mobility band was observed at increasing AlkP/QD ratios (white arrow), though the majority of QDs were not bound by AlkP despite an excess of 12 AlkP/QD. (B) EMSA images of bare QD525 with increasing ratios of AlkP/QD at pH 9.0 (top) and with 0 or 8 AlkP/QD at pH ranging from 7.0 to 9.0 (bottom). For samples prepared at pH 8.5 and below, all samples showed a distinct low mobility band in the presence of 8 AlkP/QD, indicating efficient conjugation of AlkP to QDs. At pH of 8.0 and below, no free QD band was observed in the presence of 8 AlkP/QD. The lack of a low mobility band at pH 9.0 was attributed to the high net negative charge of dimeric alkaline phosphatase at pH 9.0 which likely hindered conjugation to QDs through electrostatic repulsion with the negatively charged CL4 surface ligands.

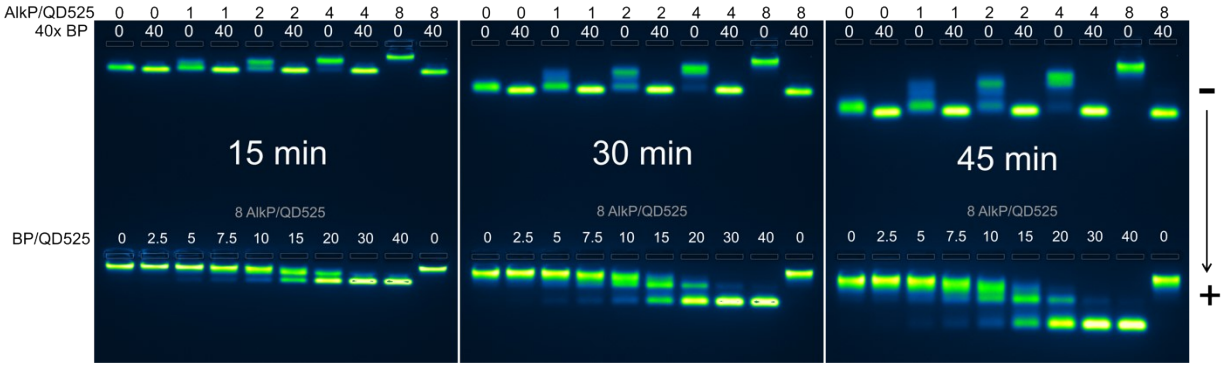

Figure S8 – Agarose EMSA images of AlkP/QD525 conjugates with and without H_6GWD_2 blocking peptides. Samples were prepared in 50 mM HEPES at pH 7.5 and run in a 1.5% agarose gel with the same buffer at 7 V/cm. Images were acquired at 15 min (left), 30 min (middle), and 45 min (right). All images were pseudocolored for visualization.

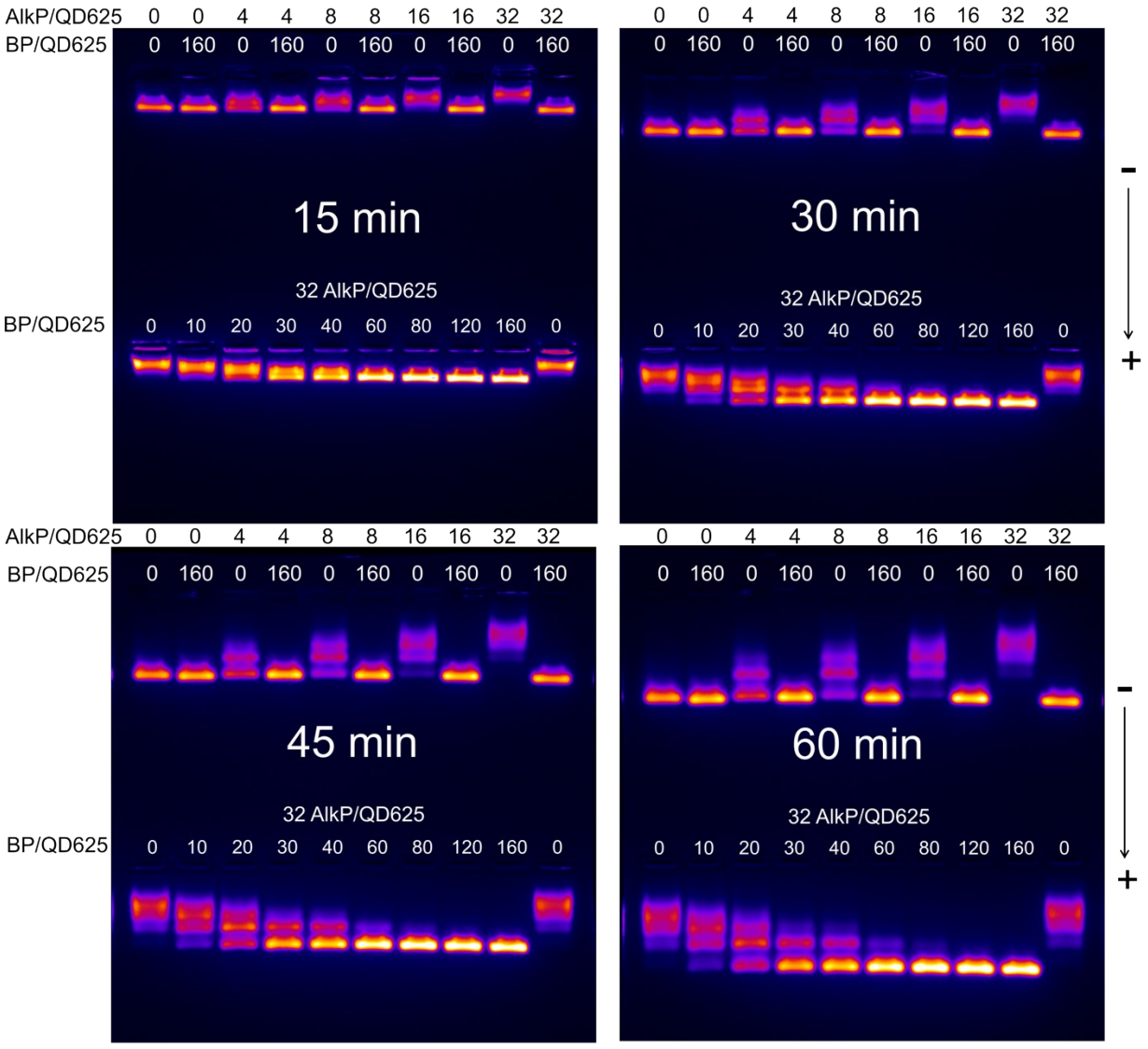

Figure S9 – Agarose EMSA images of AlkP/QD625 conjugates with and without H_6GWD_2 blocking peptides. Samples were prepared with freshly ligand-exchanged QDs in 50 mM HEPES at pH 7.3 and run in a 1.5% agarose gel with the same buffer at 7 V/cm. Images were acquired at 15 min (top left), 30 min (top right), 45 min (bottom left), and 60 min (bottom right). All images were pseudocolored for visualization.

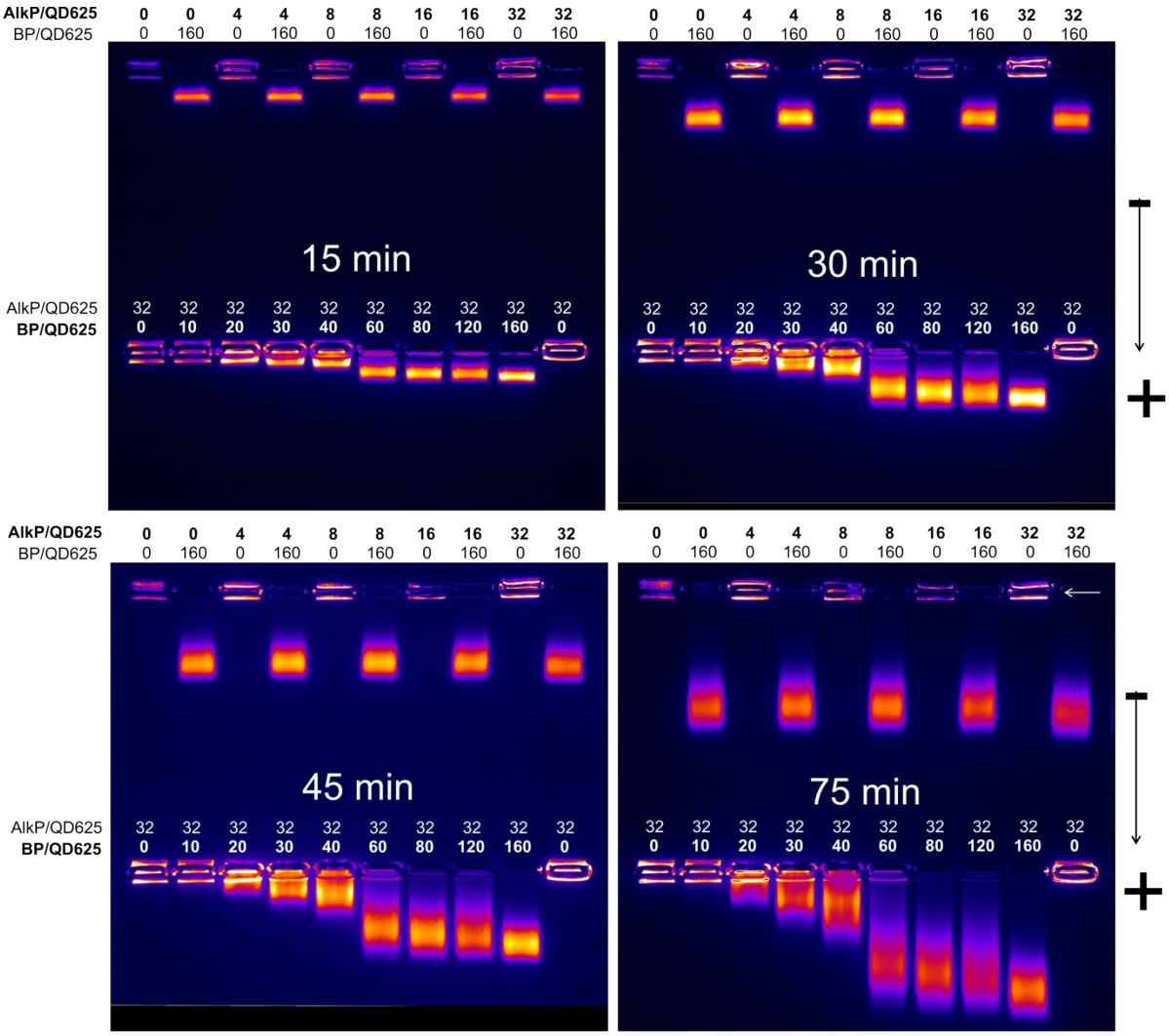

Figure S10 – Agarose EMSA images of aggregated AlkP/QD625 conjugates with and without H_6GWD_2 BPs, run at 7 V/cm in a 1.5% agarose gel. Samples were prepared and run in 50 mM HEPES at pH 7.3, and images were acquired at 15 min (top left), 30 min (top right), 45 min (bottom left), and 75 min (bottom right). Images were psuedocolored for visualization. All QD samples without BPs were found to aggregate in the wells, while QDs passivated with BPs at ratios of 60 to 160 BP/QD were colloidally stable. Aggregation was attributed to the use of an aged stock of QD625 which had been ligand-exchanged with the CL4 ligand and stored in water at 4 ºC for several months prior to use. Interestingly, the addition of H_6GWD_2 blocking peptides restored the colloidal stability of the aged QDs.

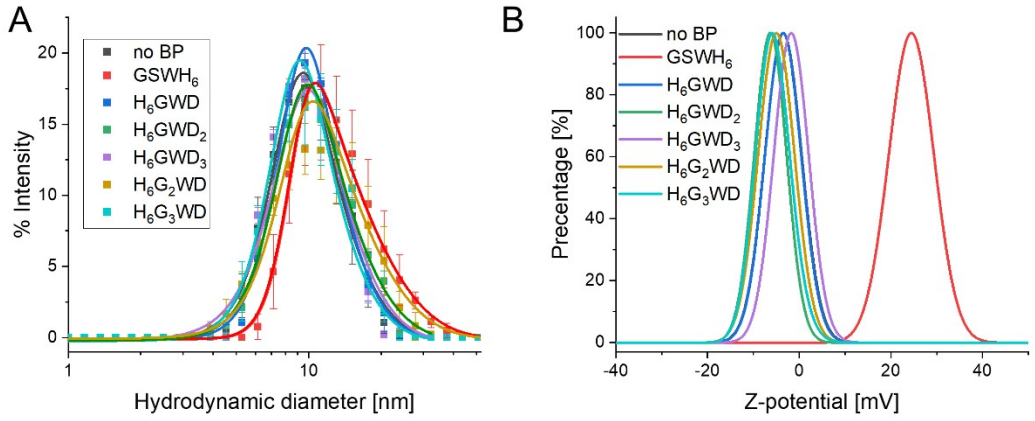

Figure S11: DLS and Z-potential were obtained on a Malvern Zetasizer Ultra. QD samples containing BP were prepared at a ratio of 40 BP/QD then diluted to 50 nM in pure water, diluting the buffer by 20-fold, and filtered through 0.2 µm filters before measuring. All samples obtained in triplicate. A) DLS data of QDs. Fits are modified gaussians to account for the tail. B) Qualitative fits of the Z-potential data for bare QDs and QDs with each of the blocking peptides.

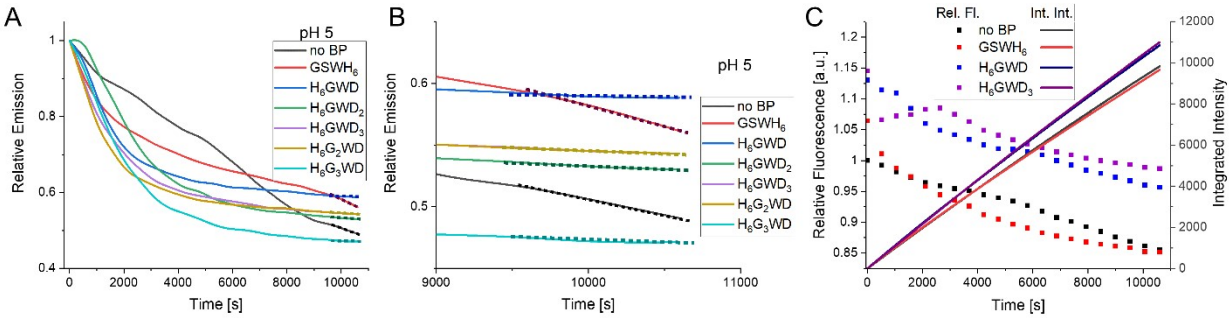

Figure S12: Representative data from stability observations. A) Relative emission, t=0 is set to 1.0, of the varying QD samples at pH 5.0 as a function of time. Data repeated from main text Figure 5C. New: dotted lines represent slope at 3 hours. B) Zoom of data from (A). These slopes along with the pH 4.5 results compose the data set for Figure 5F from main text. C) Representative data showing the relative fluorescence (data partially repeated from Figure 5D) as a function of time (squares) along with the integrated intensity (lines). The integrated intensity values, along with similar results for other BP and pH, compose the results shown in Figure 5E from main text.

References

1. K. Susumu, E. Oh, J. B. Delehanty, J. B. Blanco-Canosa, B. J. Johnson, V. Jain, W. J. t. Hervey, W. R. Algar, K. Boeneman, P. E. Dawson and I. L. Medintz, *J. Am. Chem. Soc.*, 2011, **133**, 9480-9496.
2. C. M. Green, J. Spangler, K. Susumu, D. A. Stenger, I. L. Medintz and S. A. Díaz, *ACS Nano*, 2022, **16**, 20693-20704.
3. J. C. Claussen, A. Malanoski, J. C. Breger, E. Oh, S. A. Walper, K. Susumu, R. Goswami, J. R. Deschamps and I. L. Medintz, *J. Phys. Chem. C*, 2015, **119**, 2208-2221.
4. M. Varadi, S. Anyango, M. Deshpande, S. Nair, C. Natassia, G. Yordanova, D. Yuan, O. Stroe, G. Wood, A. Laydon, A. Žídek, T. Green, K. Tunyasuvunakool, S. Petersen, J. Jumper, E. Clancy, R. Green, A. Vora, M. Lutfi, M. Figurnov, A. Cowie, N. Hobbs, P. Kohli, G. Kleywegt, E. Birney, D. Hassabis and S. Velankar, *Nucleic Acids Res.*, 2021, **50**, D439-D444.
5. J. Jumper, R. Evans, A. Pritzel, T. Green, M. Figurnov, O. Ronneberger, K. Tunyasuvunakool, R. Bates, A. Žídek, A. Potapenko, A. Bridgland, C. Meyer, S. A. A. Kohl, A. J. Ballard, A. Cowie, B. Romera-Paredes, S. Nikolov, R. Jain, J. Adler, T. Back, S. Petersen, D. Reiman, E. Clancy, M. Zielinski, M. Steinegger, M. Pacholska, T. Berghammer, S. Bodenstein, D. Silver, O. Vinyals, A. W. Senior, K. Kavukcuoglu, P. Kohli and D. Hassabis, *Nature*, 2021, **596**, 583-589.